

# Anisotropic thermal expansion in the silicate $\beta$ -eucryptite: A neutron diffraction and density functional study

A. I. Lichtenstein and R. O. Jones

*Institut für Festkörperforschung, Forschungszentrum Jülich, D-52425 Jülich, Germany*

H. Xu and P. J. Heaney

*Department of Geosciences, Princeton University, Princeton, New Jersey 08544*

(Received 22 December 1997)

The highly anisotropic thermal expansion in the hexagonal silicate  $\beta$ -eucryptite [ $\beta$ -LiAlSiO<sub>4</sub>] has been investigated using neutron diffraction measurements (for temperatures from 20 to 873 K) and density functional calculations. The agreement between theory and experiment is very good, and the main features of the expansion can be explained by anomalies in the phonon spectrum. The low- $T$  minimum of the lattice constant perpendicular to the hexagonal axis can be attributed to an additional “chemical invar” mechanism arising from the double-well energy surface of the Li ions that is also evident in the order-disorder transition in the material. [S0163-1829(98)04134-4]

## I. INTRODUCTION

Thermal expansion is a basic property of any material, and *differences* in thermal-expansion coefficients are important in many fields. Examples are the weathering of rocks, the stability of alloys under heat treatment, and the use of glazes in ceramics. Thermal expansion determines the ultimate usefulness of many ceramics, and large optical instruments—such as telescope mirrors—provide examples where low thermal expansion over a range of temperatures is essential.<sup>1</sup> The hexagonal aluminosilicate  $\beta$ -eucryptite (LiAlSiO<sub>4</sub>) (Ref. 2) has remarkable thermal-expansion properties, with coefficients that are extremely anisotropic ( $\alpha_a \sim 8.6 \times 10^{-6} \text{ deg}^{-1}$ ;  $\alpha_c \sim -18.4 \times 10^{-6} \text{ deg}^{-1}$ ) and almost independent of temperature in the range 300–1400 K.<sup>3</sup> The relationship  $\alpha_c \approx -2\alpha_a$  suggests that polycrystalline or glassy phases should have a low “average” volume thermal expansion in this temperature range. Polycrystalline  $\beta$ -eucryptite is, in fact, a major component of modern ceramic stove tops.<sup>1,2</sup>

This material is also a subject of continuing interest to earth scientists, due to its structural similarity to  $\beta$ -quartz. Quartz is the most common oxide in the earth’s crust, and studies of  $\beta$ -eucryptite shed light on the structural behavior of  $\beta$ -quartz, which cannot be quenched below 573 °C and is difficult to investigate. Furthermore, many minerals in nature experience impurity-induced phase transitions in which dopants mimic the effects of changing temperature. The substitution of LiAl for Si in quartz is a classic example of such a transition, and studies on  $\beta$ -eucryptite should help clarify the role that dopants play in the  $\alpha$ - $\beta$  phase transition in quartz.

Thermal expansion has been studied in many simple crystals. An example is Si, with two atoms in the unit cell, where anomalies in the Grüneisen parameters for zone-boundary transverse-acoustic phonons contribute to the negative (isotropic) thermal expansion at low  $T$ .<sup>4</sup> The situation is much more complicated in  $\beta$ -eucryptite, whose (average) high- $T$  structure with space group  $P6_222$  is shown in Fig. 1. This is

a lithium-stuffed derivative of high quartz ( $\beta$ -SiO<sub>2</sub>),<sup>2</sup> comprising parallel double helices of SiO<sub>4</sub> and AlO<sub>4</sub> tetrahedra. The alternation of layers containing Si and Al atoms results in a doubling of the  $c$  axis of  $\beta$ -quartz. There are one-dimensional channels along this axis that are occupied by Li<sup>+</sup> ions, which compensate the charge imbalance of the Si<sup>4+</sup> and Al<sup>3+</sup> ions and show both one-dimensional superionic conductivity<sup>5</sup> and an order-disorder transition near 755 K.<sup>6</sup> Below this temperature, the Li<sup>+</sup> ions form a superstructure occupying sites in the Si and Al planes in the ratio 3:1.<sup>7</sup> While it is plausible that the thermal expansion in  $\beta$ -eucryp-

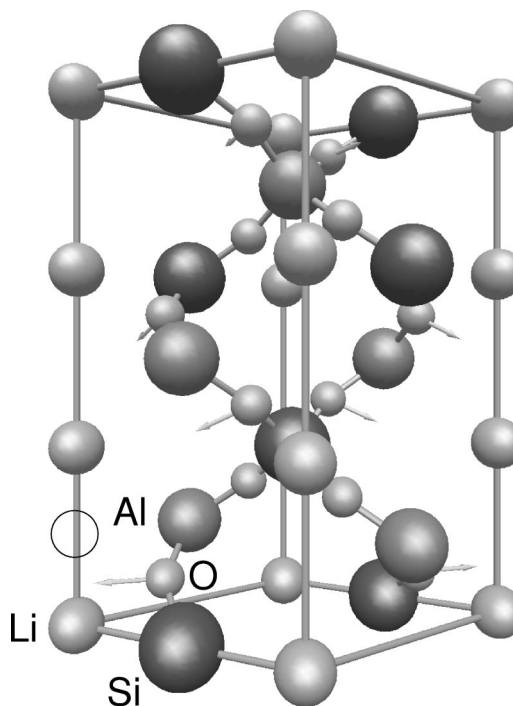


FIG. 1. “Average” structure of  $\beta$ -LiAlSiO<sub>4</sub> and the phonon eigenvectors for a typical bending mode. The circle shows the site of a “second” local minimum in the energy surface.

tite is highly anisotropic,<sup>2</sup> our understanding of this material—experimental and theoretical—is far from complete.

We describe here neutron-diffraction determinations of the lattice constants for temperatures between 20 and 873 K as well as calculations of the expansion coefficients. The measurements provide data on the low-temperature thermal behavior of  $\beta$ -eucryptite (from 20 to 300 K). Moreover, our unit-cell parameter data are based on whole-pattern fitting of powder diffraction and are more accurate than earlier work based on a least-squares analysis of a comparatively small number of diffraction lines. The calculations use a density functional (DF) method that is free of adjustable parameters. The negative thermal expansion is shown to be related to both the existence of phonons with negative Grüneisen parameters and the unusual behavior of the Li atoms described above.

## II. NEUTRON DIFFRACTION MEASUREMENTS

$\beta$ -eucryptite was synthesized from  $\text{Li}_2\text{CO}_3$ ,  $\text{Al}_2\text{O}_3$ , and  $\text{SiO}_2 \cdot n\text{H}_2\text{O}$  powders in the molar ratio 1:1:2. The mixture was sintered in a Deltech vertical-tube furnace at 1100 °C for 15 h and, after grinding, resintered at 1300 °C for 24 h. X-ray diffraction showed that the final material consisted only of  $\beta$ -eucryptite. Low- and high-temperature time-of-flight (TOF) neutron-diffraction experiments were carried out at the Manuel Lujan, Jr. Neutron Scattering Center (MLNSC) at the Los Alamos National Laboratory. The data at 20, 100, and 200 K were collected on the high intensity powder diffractometer (HIPD), and those at 298, 543, 748, and 873 K with the neutron powder diffractometer (NPD). The HIPD data were collected in four detector banks centered at  $\pm 90^\circ 2\theta$  and  $\pm 151^\circ 2\theta$ , and the NPD data in two banks centered at  $\pm 90^\circ 2\theta$ . Data from two banks were analyzed simultaneously at each temperature.

Rietveld refinement was performed using the general structure analysis system<sup>8</sup> with starting atomic parameters from Ref. 7. The parameters were refined as follows. After converging scale factor and three background terms, specimen displacement and lattice parameters were added and optimized. Between 3 and 12 background terms were added for each histogram, and the peak profiles fitted by refining isotropic and anisotropic broadening parameters in a TOF profile function.<sup>9</sup> In the final cycle, atomic positions and temperature factors of Li, Si, Al, and O were refined using 37–54 variational parameters, leading to  $R_{wp}$  values ranging from  $\sim 6\%$  (low- $T$  data) to  $\sim 13\%$  (high- $T$  data). The lattice constants for all temperatures are given in Table I. The volume expansion coefficient is small and negative for these temperatures.

## III. DENSITY FUNCTIONAL CALCULATIONS

### A. Structures

The DF calculations were performed with the local-density approximation for the exchange-correlation energy, a plane-wave basis with a kinetic energy cutoff of 70 Ry, and nonlocal pseudopotentials to represent the electron-ion interactions.<sup>10</sup> The low- $T$  structure has twelve formula units (84 atoms) in the unit cell. Optimization with respect to vol-

TABLE I. Lattice constants obtained from neutron diffraction data. The estimated standard deviations of the last digits are given in brackets.

$T$ (K)	$a$ (Å)	$c$ (Å)
20	10.4894 (3)	11.2227 (4)
100	10.4883 (3)	11.2167 (4)
200	10.4884 (4)	11.2032 (5)
298	10.4940 (1)	11.1921 (1)
523	10.5184 (3)	11.1544 (4)
748	10.5417 (4)	11.1081 (4)
873	10.5539 (2)	11.0821 (2)

ume  $V$  and  $c/a$  ratio (relaxing all internal degrees of freedom) leads to a hexagonal structure with lattice constants (relative to the experimental values)  $a = 0.98a_{\text{exp}}$ ,  $c = 1.00c_{\text{exp}}$ . As the temperature is increased, there is a progressive disordering of the Li distribution, with a phase transition to a smaller unit cell.<sup>2</sup> The “average” structure of  $\beta$ -eucryptite at high temperatures has three formula units (21 atoms) in the unit cell, with all Li atoms in the Si layers. For this structure, we find  $a = 1.01a_{\text{exp}}$ ,  $c = 1.00c_{\text{exp}}$ . As expected, the low- $T$  structure is more compact than the high- $T$  structure.

The  $\text{Li}^+$  ions in the low- $T$  structure can occupy sites with tetrahedral oxygen coordination in both the Al and Si planes. Using the lattice constants found for the 3:1 supercell structure, we have optimized the 2:2 and 4:0 structures allowing *all* internal coordinates to relax. Relative to the energy of the 3:1 structure, the 2:2 form lies 15 meV (170 K) and the 4:0 supercell 55 meV (600 K) per unit cell of the high- $T$  structure (three Li atoms) higher. These results are consistent with the 3:1 structure found at low temperatures and are in qualitative agreement with the observed order-disorder critical temperature ( $\sim 750$  K).

The barriers between the different energy minima for Li structures is crucial for discussing the ionic conductivity of  $\beta$ -eucryptite, which is 3–4 orders of magnitude greater along the hexagonal axis than in the  $ab$  plane.<sup>5</sup> We have studied the energy barriers for diffusion in the  $c$  direction of one ( $\text{Li}_1$  in Fig. 2) and three Li atoms per cell ( $\text{Li}_3$ ), respectively. We have used the “average” structure and allowed the positions of *all* other atoms to relax fully. Figure 2 shows that the barrier for correlated Li motion ( $\sim 0.3$  eV per Li atom) is much less than the energy required for uncorrelated hopping ( $\sim 0.8$  eV). The experimental thermal activation energy is 0.79 eV,<sup>5</sup> and the degree of correlation has been estimated from diffuse neutron-scattering measurements to be  $19 \pm 3$  atoms.<sup>6</sup> To see whether the calculated barrier (Fig. 2) is consistent with the latter finding, we have performed a Monte Carlo calculation at 1000 K for this barrier. The half width of the resulting structure factor distribution ( $0.06 2\pi/c$ ) corresponds to a Li correlation length of  $\sim 17$  atoms, in good agreement with the neutron-scattering data of Ref. 6.

### B. Thermal expansion

#### 1. Formalism

The thermal expansion of an anisotropic crystal with elastic deformation  $u_i$ , temperature  $T$ , and volume  $V$  can be determined from the free energy<sup>11</sup>

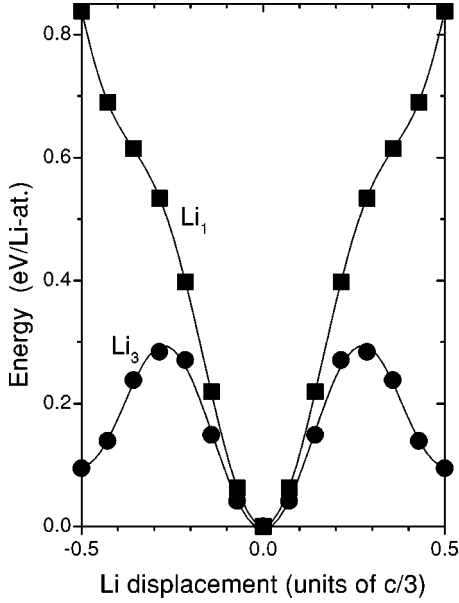


FIG. 2. Energy barrier for Li diffusion in  $\beta$ -eucryptite.  $\text{Li}_1$  (squares): energy change on moving one Li atom along the  $c$  axis;  $\text{Li}_3$  (circles): energy change on moving all three Li atoms. A displacement of 0.5 in units of  $c/3$  is half the distance to the next Li atom.

$$F(u_i, T) = E(0,0) + \frac{1}{2} V \sum_{i,j} B_{ij} u_i u_j + F^*(u_i, T),$$

where  $E(0,0)$  is the ground-state total energy,  $V$  is the volume,  $B_{ij}$  the elastic compliances, and  $F^*$  is the temperature-dependent part. In the absence of stresses, the equilibrium values of  $u_i$  can be determined from  $\partial F/\partial u_i = 0$ , yielding the thermal-expansion coefficients  $\alpha_i = du_i/dT = \sum_j (B^{-1})_{ij} \partial S/\partial u_j$ , where the entropy  $S = -\partial F^*/\partial T$ .

For a uniaxial crystal such as  $\beta$ -eucryptite, we define independent volume and tetragonal deformations  $du_1 = d\ln V$  and  $du_2 = d\ln(c/a)$ . Within the quasiharmonic approximation, where the vibrations are assumed to be harmonic but with deformation-dependent frequencies, the anisotropic thermal expansion can then be written as<sup>11</sup>

$$\alpha_a(T) = \frac{1}{3BB_{22}} [(B_{22} + B_{12})\gamma_1 - (B_{11} + B_{12})\gamma_2], \quad (1)$$

$$\alpha_c(T) = \frac{1}{3BB_{22}} [(B_{22} - 2B_{12})\gamma_1 + (2B_{11} - B_{12})\gamma_2].$$

The bulk modulus  $B$  and the compliances  $B_{ij}$ , which are related by  $B = B_{11} - B_{12}^2/B_{22}$ , can be calculated from the energy surface at  $T=0$ . The results<sup>12</sup> agree well with the experimental values<sup>13</sup> (shown in brackets):  $B = 1.21(1.03)$  Mbar,  $B_{11} = 1.22(1.04)$  Mbar,  $B_{22} = 0.38(0.35)$  Mbar,  $B_{12} = -0.02(-0.07)$  Mbar. The temperature dependence arises from the Grüneisen parameters  $\gamma_i (i=1,2)$ :

$$\gamma_i(T) = - \sum_{\mathbf{q}n} \frac{\partial \omega_n(\mathbf{q})}{\partial u_i} \frac{\partial n_B[\omega_n(\mathbf{q})]}{\partial T},$$

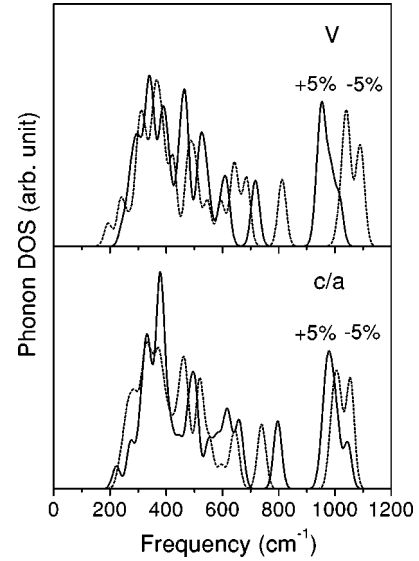


FIG. 3. Dependence of phonon spectrum on volume  $V$  (upper curve) and  $c/a$  ratio (lower curve). Full curve: 5% expansion; dashed curve: 5% contraction. We use a broadening of  $20 \text{ cm}^{-1}$  for each mode.

where  $n_B(\omega) = [\exp(\hbar\omega/k_B T) - 1]^{-1}$  is the Bose-Einstein function. The frequencies  $\omega_j(\mathbf{q})$ —the  $j$ th branch of the phonon spectrum with wave vector  $\mathbf{q}$ —are determined from the eigenvalues of the dynamical matrix  $(\mathbf{D} - \omega^2 \mathbf{I})\mathbf{C} = \mathbf{0}$ , where  $D_{\alpha\beta} = (1/\sqrt{M_\alpha M_\beta}) \partial^2 E / \partial R_\alpha \partial R_\beta$  and  $\mathbf{I}$  is the unit matrix. The phonon contribution to thermal expansion can then be found by calculating all phonon frequencies and their derivatives with respect to  $V$  and  $c/a$ .<sup>14</sup>

$$\frac{\partial \omega_n}{\partial u_i} = \frac{1}{2\omega_n} \sum_{\alpha\beta} C_{\alpha n}^* \frac{\partial D_{\alpha\beta}}{\partial u_i} C_{\beta n}.$$

## 2. Phonon spectrum

Density functional calculations of the phonon spectrum are numerically demanding, and calculations of thermal expansion have been limited to date to relatively simple systems with one or two atoms in the unit cell. Here we have a complex, uniaxial structure (even the simpler high- $T$  structure has 21 atoms in the unit cell), and we require numerically accurate values of the phonon frequencies and their derivatives with respect to the (anisotropic) distortions. The high- $T$  structure has 60 optic modes and 3 acoustic modes at the  $\Gamma$  point, and the dispersion of the phonon branches should be small. This is in contrast to the situation in silicon, for example, where the contribution of zone-boundary phonons is important.<sup>4</sup> We have calculated the phonon spectra for the high- $T$  and low- $T$  structures of  $\beta$ -eucryptite, with 3 and 12 formula units, respectively. Our finding that the phonon spectra are very similar supports our assumption that phonon dispersion is weak in this material.

The phonon spectra calculated assuming no dispersion (i.e.,  $q=0$ ) are shown in Fig. 3 for the high- $T$  structure and for changes in the  $c/a$  ratio and volume  $V$  of  $\pm 5\%$ . There are prominent peaks in the phonon density of states near 400, 600–800, and 1000  $\text{cm}^{-1}$ . The  $c/a$  Grüneisen parameters ( $\gamma_2$ ) for modes around 400  $\text{cm}^{-1}$  (“bending” Si-O and

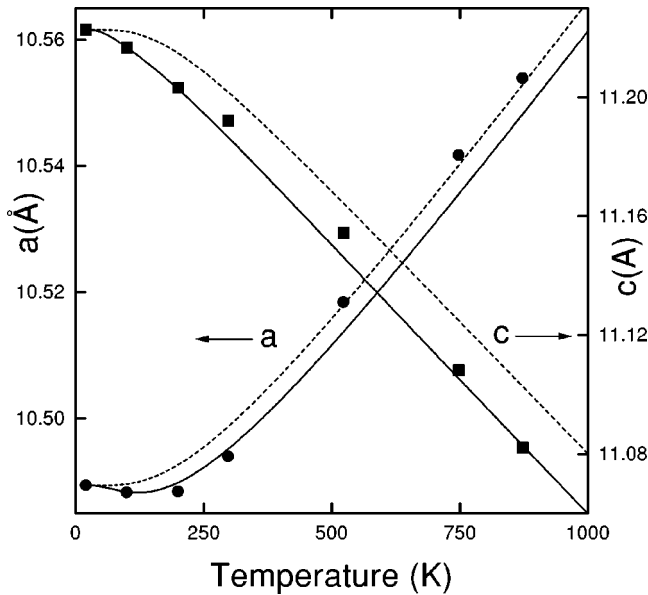


FIG. 4. Temperature dependence of lattice constants  $a$  (left scale, experiment: circles) and  $c$  (right scale, experiment: squares) in  $\beta$ -eucryptite. Dashed curves: phonon mechanism alone, full curves: including effects of the “two-level” system. The theoretical lattice constants at  $T=0$  are set equal to the experimental values.

Al-O modes, eigenvectors of a typical phonon are shown in Fig. 1) are strongly negative, as are some of the modes around  $800\text{ cm}^{-1}$ , while phonons near  $1000\text{ cm}^{-1}$  (“stretching” Si-O and Al-O modes) have normal (positive) Grüneisen parameters. Apart from the lowest frequency phonons in Fig. 3, the volume Grüneisen parameters are positive, i.e., the frequencies are higher for the compressed structure. The nontrivial cancellation of the contributions to thermal expansion of phonons up to  $800\text{ cm}^{-1}$  and around  $1000\text{ cm}^{-1}$  results in a small average volume expansion. Since  $|B_{11}\gamma_2| > |B_{22}\gamma_1|$  and all combinations of elastic constants in the brackets of Eq. (1) are positive,  $\alpha_a$  and  $\alpha_c$  have opposite signs. The calculated temperature dependence of the lattice constants  $a$  and  $c$  agree remarkably well with experiment (Fig. 4, dashed curve), as do the high-temperature values of  $\alpha_a (9.46 \times 10^{-6}\text{ deg}^{-1})$  and  $\alpha_c (-17.7 \times 10^{-6}\text{ deg}^{-1})$ .

It is interesting to compare the situation with that in silica, where there is a network of neutral  $\text{SiO}_4$  tetrahedra and the negative thermal expansion is related to the low-frequency phonons that are responsible for the  $\alpha$ - $\beta$  phase transition. For  $\beta$ -quartz there are such rigid unit modes<sup>15</sup> for  $\mathbf{q}$  at high symmetry points in the Brillouin zone (BZ), in the (001) plane, and along the [001] directions.<sup>16</sup> One mode at the  $\Gamma$  point is a soft mode of the displacive transition, and it has a frequency of only  $\sim 30\text{ cm}^{-1}$  even for  $T \sim 1200\text{ K}$ . The presence of low-frequency phonons and the distribution of weight over the BZ dominate the expression for  $\gamma_i$ , due to the approximate  $1/\omega_n^2$  dependence and the large thermal factor  $\partial n_B / \partial T$ . The corresponding modes in  $\beta$ -eucryptite have much higher frequencies ( $\sim 200\text{ cm}^{-1}$ ), due to the large electrostatic potentials arising from the effective multilayers of Al and Si-Li. Since  $\partial n_B / \partial T$  changes only by a factor of 3–5 for temperatures between 300 and 1400 K and phonons

in the range  $200\text{--}1200\text{ cm}^{-1}$ , all modes contribute to thermal expansion.

### C. A “chemical invar” effect?

The precision of the present measurements allows us to identify unambiguously the presence of a minimum in  $a(T)$  (Fig. 4). The calculations based on the phonon mechanism do not show this feature, and it is interesting to speculate on its origin. We have noted the existence of a two-level system involving the motion of the Li atoms, and calculations on the “average” structure show that both the  $c$  and  $a$  axes are  $\sim 1\%$  shorter for the higher-energy minimum at the Al plane (Fig. 2). There is an obvious analogy to the invar effect in  $\text{Fe}_3\text{Ni}$  alloys, where a less stable nonmagnetic state is more compact than the magnetic ground state<sup>17</sup> and increasing the temperature and the population of the higher-energy state leads to contraction.

This mechanism is related to the order-disorder phase transition in the Li subsystem in  $\beta$ -eucryptite, and it could lead to a negative contribution to the thermal expansion. To estimate its order of magnitude, we have studied a simple two-level model used previously in the invar case.<sup>17</sup> If we adopt the contracted values of the lattice constants mentioned above and an energy difference between the two structures of 500 K, we can estimate the correction arising from this mechanism. The result, shown as the full curves in Fig. 4, is in improved agreement with experiment. While these results show that the existence of a “chemical invar” mechanism in  $\beta$ -eucryptite is plausible, other contributions—such as those from the  $q \neq 0$  phonons—must be estimated before firm conclusions can be drawn. We are extending the present calculations to include these effects.

## IV. DISCUSSION AND CONCLUDING REMARKS

$\beta$ -eucryptite is a unique material. It has a uniaxial crystalline structure closely related to that of  $\beta$ -quartz and is a “one-dimensional” superionic conductor with an order-disorder phase transition. Its polycrystalline, glass ceramic form has a small (and negative) thermal-expansion coefficient over a large temperature range. We have presented here neutron-diffraction data for the thermal expansion of a polycrystalline sample for  $20\text{ K} < T < 873\text{ K}$ , and we are performing x-ray-diffraction studies of the same sample at the same temperatures to refine the structure further.

The density functional calculations described here provide a remarkably good description of the energy surfaces and related properties of an interesting material with a complex structure. The agreement between theory and experiment for the thermal expansion is particularly encouraging, since such calculations must incorporate both the quantum nature of the phonons and an accurate estimate of their frequencies. The quasiharmonic approximation we have used is not appropriate at very high temperatures, but there is no sign that it does not hold in the temperature range of the present measurements on  $\beta$ -eucryptite. The identification of the origin of the unusual behavior of this material should stimulate the search for other materials with similar properties.

## ACKNOWLEDGMENTS

We thank R. von Dreele and M. Bourke for kindly collecting the neutron diffraction data, P. Ballone, U. Fotheringham, V. Heine, M. Katsnelson, P. Nielaba, and C. Rickwardt for helpful discussions, and G. K. White for comments on the original manuscript. The work was supported by the MaTech Program of the BMBF, Bonn (03N8008E0, A.L.),

the NSF (EAR9706143, P.J.H.), and the 1996 and 1997 ICDD Crystallography Scholarships (H.X.) and was carried out in part at the Los Alamos Neutron Science Center (LANSCE). The Los Alamos National Laboratory is supported by the U.S. Department of Energy. The calculations were performed on Cray T3E computers in the Forschungszentrum Jülich with grants of CPU time from the Forschungszentrum and the German Supercomputer Center (HLRZ).

- 
- <sup>1</sup>See, for example, *Low Thermal Expansion Glass Ceramics*, edited by H. Bach, Schott Series on Glass and Glass Ceramics (Springer, Berlin, 1995).
- <sup>2</sup>See, for example, D. C. Palmer, in *Silica. Physical Behavior, Geochemistry, and Materials Applications*, edited by P. J. Heaney, C. T. Prewitt, and G. V. Gibbs, Reviews in Mineralogy, Vol. 29 (Mineralogical Society of America, Washington, D.C., 1996), p. 83.
- <sup>3</sup>W. W. Pillars and D. R. Peacor, *Am. Mineral.* **58**, 681 (1973). Earlier measurements produced very similar results: F. H. Gilgery and E. A. Bush, *J. Am. Ceram. Soc.* **42**, 175 (1959)(8.21, -17.6); T. Y. Tien and F. A. Hummel, *ibid.* **47**, 582 (1964) (8.11, -16.9). ( $\alpha_a$ ,  $\alpha_c$  in units of  $10^{-6}$  deg $^{-1}$ .)
- <sup>4</sup>See, for example, S. Biernacki and M. Scheffler, *Phys. Rev. Lett.* **63**, 290 (1989); C. H. Xu, C. Z. Wang, C. T. Chan, and K. M. Ho, *Phys. Rev. B* **43**, 5024 (1991), and references therein.
- <sup>5</sup>D. M. Follstaedt and P. Richards, *Phys. Rev. Lett.* **37**, 1571 (1976).
- <sup>6</sup>W. Press, B. Renker, H. Schulz, and H. Böhm, *Phys. Rev. B* **21**, 1250 (1980).
- <sup>7</sup>H. Guth and G. Heger, in *Fast Ion Transport in Solids, Electrodes and Electrolytes*, edited by P. Vashishta, J. N. Mundy, and G. K. Shenoy (Elsevier, North-Holland, 1979), p. 499.
- <sup>8</sup>A. C. Larson and R. B. von Dreele, *General Structure Analysis System (GSAS)*, (Los Alamos National Laboratory Report LAUR 86-748, 1994), p. 179.
- <sup>9</sup>R. B. von Dreele, J. D. Jorgensen, and C. G. Windsor, *J. Appl. Crystallogr.* **15**, 581 (1982).
- <sup>10</sup>N. Troullier and J. M. Martins, *Phys. Rev. B* **43**, 1993 (1991). The calculations were performed with the CPMD program version 3.0, J. Hutter *et al.*, MPI für Festkörperforschung and IBM Research 1990-97.
- <sup>11</sup>E. Grüneisen and E. Goens, *Z. Phys.* **29**, 141 (1924). See also V. I. Nizhankovskii *et al.*, *Pis'ma Zh. Éksp. Teor. Fiz.* **59**, 693 (1994) [*JETP Lett.* **59**, 733 (1994)]. For an extensive review, see T. H. K. Barron, J. G. Collins, and G. K. White, *Adv. Phys.* **29**, 609 (1980).
- <sup>12</sup>The elastic compliances and stiffnesses for a hexagonal close-packed crystal are related by  $B_{11} = \frac{2}{9}(c_{11} + c_{12} + 2c_{13} + \frac{1}{2}c_{33})$ ;  $B_{22} = \frac{2}{9}(c_{11} + c_{12} - 4c_{13} + 2c_{33})$ ;  $B_{12} = \frac{2}{9}(-c_{11} - c_{12} + c_{13} + c_{33})$ .
- <sup>13</sup>S. Haussühl, W. Nagel, and H. Böhm, *Z. Kristallogr.* **169**, 299 (1984).
- <sup>14</sup>See also A. Debernardi and M. Cardona, *Phys. Rev. B* **54**, 11 305 (1996).
- <sup>15</sup>See, for example, A. P. Giddy, M. T. Dove, G. S. Pawley, and V. Heine, *Acta Crystallogr., Sect. A: Found. Crystallogr.* **49**, 697 (1993).
- <sup>16</sup>M. Vallade, B. Berge, and G. Dolino, *J. Phys. I* **2**, 1481 (1992).
- <sup>17</sup>See, for example, R. J. Weiss, *Proc. Phys. Soc. London* **82**, 281 (1963).